



## Ni/TiO<sub>2</sub> Catalysts Supported with Al<sub>2</sub>O<sub>3</sub> Over CO<sub>2</sub> Reforming†

H. SUN, Q.J. GONG, B.H. LV and J. HUANG\*

Department of Applied Chemistry, Yuncheng University, Yuncheng, Shanxi Province, P.R. China

\*Corresponding author: Fax: +86 359 2090378; Tel: +86 359 2090394; E-mail: jianhuang3@126.com

AJC-15728

The 5 wt % Ni/TiO<sub>2</sub>-Al<sub>2</sub>O<sub>3</sub> xerogels catalyst was prepared by the sol-gel synthesis of titanium *n*-butoxide in methanol with nickel and aluminum. X-Ray diffraction, TG/DTA and SEM were used to characterize the function of addition aluminum to Ni/TiO<sub>2</sub> catalyst. The role of aluminum addition promotes the formation of large metallic Ni ensembles increase the dispersion of Ni, suppression of Ni/TiO<sub>2</sub> catalyst deactivation and carbon deposition.

**Keywords:** CO<sub>2</sub>-reforming, Methane, Nickel catalysis, Aluminum, Carbon deposition.

### INTRODUCTION

Carbon dioxide reforming is meaningful because it produces a more suitable H<sub>2</sub>/CO ratio for the Fisher-Tropsch. However, this reaction has not been established industrial due to the serious catalyst deactivation. It is well known that many transition metal-based are good catalysts for the CO<sub>2</sub> reforming reaction, especially noble and Ni-based catalysts. Although noble metal catalysts show better performance than nickel, but the high cost of noble metals renders their application. Therefore, development of Ni-based catalysts with little or no carbon deposition is of great interesting to industrial application for CO<sub>2</sub> reforming.

Some researchers have stated that the addition of titanium improves the stability of these catalysts, especially inhibiting the carbon deposition. When a titanium-supported nickel was employed in catalytic CO<sub>2</sub> reforming, the catalyst showed a high initial activity but suffered instability based both on the poor reduced surface area and Ti<sub>3</sub>O<sub>5</sub> was covering the active sites of Ni catalysts.

Zhang and Reller<sup>1</sup> showed that the larger metal particles stimulated the amorphous carbon deposition because of the ensemble result which was covering the active metal surface. So solid solution formation and decorating Ni crystallites with other oxides *etc.* are proved to be effective in the elimination of large Ni metal ensemble. For instance, the formation of NiAl<sub>2</sub>O<sub>4</sub> results in the formation of small Ni crystallites which resist to carbon deposition<sup>2,3</sup>. A number of articles reported that mobile oxygen on the surface of catalysts is related to the

carbon elimination<sup>4,5</sup>. As a high temperature reaction, it is required that the catalyst has good thermal stability. The formation of NiAl<sub>2</sub>O<sub>4</sub> solid solution can improve the oxygen storage capacity, the redox property and the thermal resistance.

In this work, we reported on the study of CO<sub>2</sub> reforming over Ni/TiO<sub>2</sub>-Al<sub>2</sub>O<sub>3</sub> catalyst. It also reported an effect of adding aluminum to Ni/TiO<sub>2</sub> catalysts. The major function of an aluminum additive was to improve development of pore structure and inhibit Ti<sub>3</sub>O<sub>5</sub> formation. The best effect in securing stability without sacrificing much activity was obtained when aluminum was used as a modifying additive. In this paper, the role of aluminum oxide as a promoter in Ni/TiO<sub>2</sub>-Al<sub>2</sub>O<sub>3</sub> is discussed.

### EXPERIMENTAL

**Preparation of catalyst:** 5 wt % Ni/TiO<sub>2</sub>-Al<sub>2</sub>O<sub>3</sub> was prepared by sol-gel process from analytical-grade (Sinopharm Chemical Reagent Co., Ltd.). The precursors were Ni(NO<sub>3</sub>)<sub>2</sub>·6H<sub>2</sub>O, Ti(BuO)<sub>4</sub> and Al(NO<sub>3</sub>)<sub>3</sub>·9H<sub>2</sub>O. Methanol has been used as a solvent for precursor solution and hydrolyzate. The molar ratio of Ti/MeOH was at 0.12. Hydrolysis was catalyzed by HNO<sub>3</sub> with an acid/alkoxide ratio of 0.10 and hydrolysis ratio of 5.22. Appropriate amounts of Al(NO<sub>3</sub>)<sub>3</sub>·9H<sub>2</sub>O were added into Ti(BuO)<sub>4</sub> and Ni(NO<sub>3</sub>)<sub>2</sub>·6H<sub>2</sub>O solution in MeOH to make the gel solutions. Hydrolysis of the colloidal suspension was obtained by slowly dropping acid/alkoxide and at the same time stirring to keep the hydrolysis speed slow. A distinct lightly green gel was made where hydrolysis solution has been

†Presented at 2014 Global Conference on Polymer and Composite Materials (PCM2014) held on 27-29 May 2014, Ningbo, P.R. China

dropped into the colloidal suspension after 24 h. The gel was dried in air at 453 K for 10 h then calcined at 973 K for 10 h with a rate of 1 K/min from 298 K.

X-Ray powder diffraction patterns obtained by using Rigaku D/max 2250 diffraction equipment with  $\text{CuK}\alpha$  source at 40 kV and 100 mA.  $2\theta$  angles ranged from 20-80 with a speed of 8 °/min. SEM image was obtained on a Philips XL-30 microscope operated at 15 kV. The thermal behaviour and carbon deposited on the catalysts were obtained by a Perkin Elmer. Pyris Diamond TG/DTA equipment. The temperature was increased to 1023 K from 303 K at a rate of 5 K/min.

**Performance measurement of catalyst:** Catalytic performance measurement of  $\text{CO}_2$  reforming was conducted under atmospheric pressure with a tubular fixed-bed quartz reaction (5.6 mm i.d. 255 mm length). The reaction gases consisted of  $\text{CO}_2$ ,  $\text{CH}_4$  and  $\text{N}_2$  with the ratio of 1:1:1.8 at a GHSV of 942000  $\text{cm}^3 \text{h}^{-1} \text{g}^{-1}$ . The catalyst of 100 mg with the particle size of 60-80 meshes diluted with 0.5 g quartz sand (45-55 Mesh). The catalyst was reduced in-suit at 973 K for 2 h with a feed composition of  $\text{H}_2/\text{N}_2 = 1:2$ . The analyses of the tailgas were carried out on a Haixin GC-950 gas chromatograph equipped with a TCD detector.

## RESULTS AND DISCUSSION

**Activity and stability of catalyst:** The characteristic of catalytic was tested at 973 K with a feed gas ratio  $\text{CH}_4/\text{CO}_2$  of one. Table-1 listed that the  $\text{Ni}/\text{TiO}_2\text{-Al}_2\text{O}_3$  catalyst illustrated a high response rate initially and exhibited continuous higher stability during the 10 h. On the contrary, the  $\text{Ni}/\text{TiO}_2$  catalyst showed low activity and a rapid deactivation comparable to the  $\text{Ni}/\text{TiO}_2\text{-Al}_2\text{O}_3$  during the 10 h stream response. The significantly effect of aluminum improved the stability of catalytic. Table-2 showed the time-dependent reaction rate of  $\text{CH}_4$  over 5 wt %  $\text{Ni}/\text{TiO}_2\text{-Al}_2\text{O}_3$  catalyst with different  $\text{Al}_2\text{O}_3$  loading. As  $\text{Al}_2\text{O}_3$  content increased, the activity improved accordingly. It is observed that the reaction rate of the catalyst with 25 wt %  $\text{Al}_2\text{O}_3$  appears to be higher than that of 35 wt %  $\text{Al}_2\text{O}_3$  with time on stream. However, at the highest  $\text{Al}_2\text{O}_3$  loading (75 wt %), it showed the lowest reaction rate on stream. Overall evaluation of the effect of  $\text{Al}_2\text{O}_3$  addition is that proper content of  $\text{Al}_2\text{O}_3$  can improve the activity, but excessive  $\text{Al}_2\text{O}_3$  can easily cause catalyst deactivation. It was 50 wt %  $\text{Al}_2\text{O}_3$  loading that provides well stability.

TABLE-1

TIME-DEPENDENT REACTION RATE OF  $\text{CH}_4$  OVER 5 wt %  $\text{Ni}/\text{TiO}_2$  AND 5 wt %  $\text{Ni}/\text{TiO}_2\text{-Al}_2\text{O}_3$  CATALYSTS

Catalyst	Time (h)				
	0	2	4	6	8
$\text{Ni}/\text{TiO}_2$	83.0	56.0	42.0	38.0	32.0
$\text{Ni}/\text{TiO}_2/\text{Al}_2\text{O}_3$	125.0	129.0	128.0	129.0	132.0

Reaction condition: temperature 973 K, p = 1 atm. GHSV = 9,2000  $\text{cm}^3 \text{h}^{-1} \text{g}^{-1}$ ,  $\text{CH}_4/\text{CO}_2 = 1$ .

**Role of aluminum in  $\text{Ni}/\text{TiO}_2$ :** Aluminum addition to  $\text{Ni}/\text{TiO}_2\text{-Al}_2\text{O}_3$  over  $\text{CO}_2$  reforming was the suppression of catalyst deactivation and carbon deposition. The deactivation of Ni-based catalysts can be described to carbon deposition and nickel sintering. X-Ray powder diffraction patterns of  $\text{Ni}/\text{TiO}_2\text{-Al}_2\text{O}_3$

TABLE-2  
TIME-DEPENDENT REACTION RATE OF  $\text{CH}_4$  OVER 5 wt %  $\text{Ni}/\text{TiO}_2\text{-Al}_2\text{O}_3$  CATALYST WITH DIFFERENT  $\text{Al}_2\text{O}_3$

Cat.	Time (h)				
	0	2	4	6	8
$\text{Ni}/\text{TiO}_2/25 \text{ wt } \% \text{ Al}_2\text{O}_3$	182.0	180.0	179.0	177.0	176.0
$\text{Ni}/\text{TiO}_2/35 \text{ wt } \% \text{ Al}_2\text{O}_3$	146.0	142.0	143.0	144.0	145.0
$\text{Ni}/\text{TiO}_2/50 \text{ wt } \% \text{ Al}_2\text{O}_3$	201.0	201.0	201.0	200.0	200.0
$\text{Ni}/\text{TiO}_2/75 \text{ wt } \% \text{ Al}_2\text{O}_3$	118.0	118.0	118.0	119.0	119.0

Reaction condition: temperature 973 K, P = 1 atm, GHSV = 942000  $\text{cm}^3 \text{h}^{-1} \text{g}^{-1}$ ,  $\text{CH}_4/\text{CO}_2 = 1$ .

$\text{Al}_2\text{O}_3$  catalyst in fresh, reduced and post-reaction are presented in Fig. 1. It showed that no nickel reflection occurred on fresh Ni catalyst reduced at 973 K (Fig. 1). It indicated that the interaction between NiO and  $\text{Al}_2\text{O}_3$  was strong. There is still no pure NiO observed and nickel is present in the form of  $\text{NiAl}_2\text{O}_4$ . The XRD analyses of the fresh, reduced and post-reaction  $\text{Ni}/\text{TiO}_2\text{-Al}_2\text{O}_3$  catalysts are presented will generate more active sites, attributing to its high activity. In this research, it can be seen that the lower catalytic activities of  $\text{Ni}/\text{TiO}_2$  catalyst is possibly due to the blockage of the active sites. It suggests that the pores of this catalyst be blocked by the  $\text{Ti}_3\text{O}_5$ , which could prevent the contact between the reactants and the active sites. Some researchers have reported the coverage of active sites by  $\text{Ti}_3\text{O}_5$  was the main cause of  $\text{Ni}/\text{TiO}_2$  deactivation. The addition of aluminum can inhibit the reduction of  $\text{TiO}_2$ . It was the main reason that  $\text{Ni}/\text{TiO}_2\text{-Al}_2\text{O}_3$  could perform well much longer with a much better action than  $\text{Ni}/\text{TiO}_2$  catalyst.

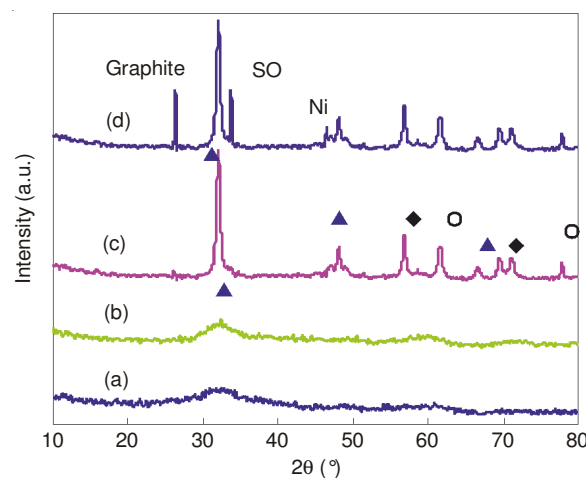


Fig. 1. X-Ray diffraction patterns for 5 wt %  $\text{Ni}/\text{TiO}_2\text{-Al}_2\text{O}_3$  catalyst. (a) Calcined at 453 K for 10 h, (b) Calcined at 773 K for 10 h, (c) Reduced at 973 K for 2 h and (d) after 120 h reaction at 973 K. ▲: Anatase; ◆: Rutile; ○:  $\text{Al}_2\text{O}_3$  or  $\text{NiAl}_2\text{O}_4$ . SO: SiO

The sample of  $\text{Ni}/\text{TiO}_2\text{-Al}_2\text{O}_3$  catalyst remained X-ray amorphous up to 453 K. It can be seen that a pure anatase phase was obtained at 773 K, it would be desirable to have a single-phase support for establishing a structure-reactivity relationship in catalytic applications. It can be seen that rutile  $\text{TiO}_2$  began to form at 973 K. It was reported that, brookite, anatase and rutile can coexist in the temperatures from 673-973 K<sup>6</sup> and  $\text{TiO}_2$  transforms to rutile between 903 and 973 K<sup>7</sup>. These results are in agreement with what the XRD presents. Rutiles was more stable and final phase of titania and anatase

transforms into rutile at 973 K. The extension of the coexistence of rutile and anatase may be due to the integration of aluminum. A existence of anatase may also contribute to the higher performance.

It can be seen that no nickel peaks in fresh catalyst due to the interaction between the metal and support Al<sub>2</sub>O<sub>3</sub> in XRD patterns. Phase transformation occurred on Al<sub>2</sub>O<sub>3</sub> supported Ni catalyst during calcination to form nickel aluminate NiAl<sub>2</sub>O<sub>4</sub> which is difficult to reduce to metallic nickel at 973 K. Assist with more porous structure has lower nickel particle size. The metallic Ni in the reduced samples preferentially forms small crystallites and the dispersion of Ni increases by adding Al<sub>2</sub>O<sub>3</sub>. The interaction among components can affect the distribution of components and the structure of the catalyst and in addition, thus affect the activity of the catalyst. Several research groups<sup>8</sup> have reported that the migration of Ni from the bulk to the surface of the catalyst may migrate to the surface during the reaction. For the XRD result (Fig. 1) Al<sub>2</sub>O<sub>3</sub> can react with the reduced NiO to form NiAl<sub>2</sub>O<sub>4</sub>. This process may promote the migration of Ni. Therefore the activity of the sample with 50 wt % Al<sub>2</sub>O<sub>3</sub> increased more quickly than the samples with different content of Al<sub>2</sub>O<sub>3</sub> (Table-2).

Tang *et al.*<sup>9</sup> reported that NiAl<sub>2</sub>O<sub>4</sub> can form after calcinations at 973 K which is easier to reduce than NiTiO<sub>3</sub>. Several researchers have found that higher calcination temperatures increase the metal-support interaction and the formation of nickel aluminum resulting in greater difficulty in reduction<sup>3,10,11</sup>. It will affect the nickel dispersion and carbon deposition. Chen and Ren<sup>3</sup> showed that carbon deposition is markedly suppressed if NiAl<sub>2</sub>O<sub>4</sub> is made. The strong interaction of the Ni-O bond in NiAl<sub>2</sub>O<sub>4</sub> results, in the formation of small Ni crystallites on the catalyst surface, which are relatively stable toward sintering and carbon deposition<sup>1</sup>.

It is known that nickel crystallites are the active sites for CO<sub>2</sub> reforming. XRD results have shown that NiAl<sub>2</sub>O<sub>4</sub> was the main phase of nickel in fresh catalyst Ni/TiO<sub>2</sub>-Al<sub>2</sub>O<sub>3</sub>. The catalyst showed higher activity and carbon resistance from nickel crystallite. Chen and Ren<sup>3</sup> also showed that NiAl<sub>2</sub>O<sub>4</sub> may be as the active site in CO<sub>2</sub> reforming. Hence, it is deduced that the reduced NiAl<sub>2</sub>O<sub>4</sub> may be an active site for this reaction exhibiting different catalytic and stability. It suggested that the calcined NiAl<sub>2</sub>O<sub>4</sub> spinel phase made not active in the reforming reaction but its reduced form could lead to a significant increase in activity and stability. It is deduced that the higher activity of Ni/TiO<sub>2</sub>-Al<sub>2</sub>O<sub>3</sub> in this research was probably due to the synergetic effect of the reduced NiAl<sub>2</sub>O<sub>4</sub> and surface nickel particles.

To the surface of the catalysts and blocked the accessibility of reacting molecules to active sites. The deactivation of Ni/TiO<sub>2</sub>-Al<sub>2</sub>O<sub>3</sub> catalysts can also be attributed to the sintering of the active phase. The result drawn from the XRD characterizations in the catalyst indicate that there is no NiO present in fresh catalyst. XRD measurements give insight into the structural changes of Ni particles and deposited carbon after the reaction. It can be seen In Fig. 1, pattern (d), shows the size Ni crystalline. The nickel crystallite phase peak on Ni/TiO<sub>2</sub>-Al<sub>2</sub>O<sub>3</sub> appeared after 120 h.

**Characterization of carbon deposits:** TG/DTA profiles of carbon deposits on the Ni/TiO<sub>2</sub>-Al<sub>2</sub>O<sub>3</sub> catalyst after 10 h

carbon are illustrated in Fig. 2. The TG mode shows a weight drop from the starting point to 542 K, it was the evaporation of moistures, methanol solvent and BuOH generated during hydrolysis and the decomposition of nitrate. The steep weight increase indicates nickel oxidized during 542-738 K. Then the weight gradually decreased until leveling off at 973 K and then shows no further weight loss (Fig. 2). The oxidation of carbonaceous species starts at 807 K, showing a maximum at 834 K, which is in agreement with the formation of filamentous carbon species, this conforms to the result of XRD. There are two types of carbon, deactivating (amorphous carbon) and non-deactivating (graphite) were found<sup>3,12</sup>. The morphology of graphitic carbon is that of carbon filaments. Chen and Ren<sup>3</sup> reported that the filamentous carbon with a hollow inner channel would form on the surface of 10 wt % Ni/6-Al<sub>2</sub>O<sub>3</sub> catalysts. They did not lose their activity in tests for as long as 120 h.

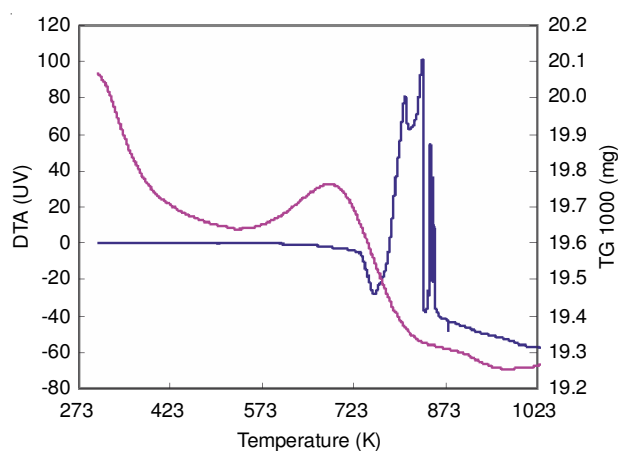


Fig. 2. TG/DTA profiles of 5 wt % Ni/TiO<sub>2</sub>-Al<sub>2</sub>O<sub>3</sub> catalyst after 10 h reaction. Reaction condition: temperature 974 K, P = 1 atm, CH<sub>4</sub>/CO<sub>2</sub> = 1 GHSV = 942000 cm<sup>3</sup> h<sup>-1</sup> g<sup>-1</sup>

Fig. 3 illustrates the SEM micrograph of the Ni/TiO<sub>2</sub>-Al<sub>2</sub>O<sub>3</sub> catalyst showing the well-surface area and mesoporous.

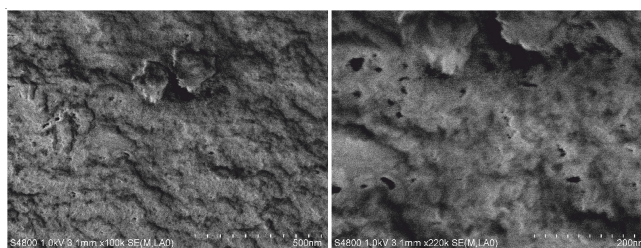


Fig. 3. SEM micrograph of the Ni/TiO<sub>2</sub>-Al<sub>2</sub>O<sub>3</sub> catalyst illustrating well-surface area and mesoporous

Carbon deposition on Ni/TiO<sub>2</sub>-Al<sub>2</sub>O<sub>3</sub> catalyst is mainly graphitic as shown in XRD. It can be seen that the peak of graphitic carbon appears in Ni/TiO<sub>2</sub>-Al<sub>2</sub>O<sub>3</sub> after CO<sub>2</sub> reforming for 120 h. The foregoing discussions have shown that graphitic carbon is more active in the CO<sub>2</sub> reforming, probably due to its close contact with nickel particles. Therefore, Ni/TiO<sub>2</sub>-Al<sub>2</sub>O<sub>3</sub> catalyst showed higher stability in this reaction, because of its more active carbon species. This behaviour may be attributed to the formation of NiAl<sub>2</sub>O<sub>4</sub>. It was reported that NiAl<sub>2</sub>O<sub>4</sub> solid solution could minimize the Ni particle size to suppress the carbon formation<sup>3</sup>. It is expected that the Al<sub>2</sub>O<sub>3</sub> addition to

Ni/TiO<sub>2</sub> can modify the Ni ensembles environment by the Ni-Al alloy formation. Hence, the Al<sub>2</sub>O<sub>3</sub> addition effects the Ni/TiO<sub>2</sub> catalyst to suppress the carbon deposition during CO<sub>2</sub> reforming. Although the amount of carbon deposition on the Ni/TiO<sub>2</sub>-Al<sub>2</sub>O<sub>3</sub> catalyst was appeared, the catalyst kept high activity with reaction rate as shown in Table-1. The amount of carbon deposition was not always to the catalyst deactivation. Chen and Ren<sup>3</sup> reported that the carbon deposition on the NiAl<sub>2</sub>O<sub>4</sub> spinel was markedly suppressed during the CO<sub>2</sub> reforming. Their results agreed with our results during the reaction time till 120 h in the carbon deposition on the Ni/TiO<sub>2</sub>-Al<sub>2</sub>O<sub>3</sub> catalyst. Hence, the deactivation of Ni/TiO<sub>2</sub>-Al<sub>2</sub>O<sub>3</sub> catalyst has been ascribed to Ni sintering. The presence of a nickel phase in the XRD pattern of used catalyst after 120 h reaction indicates that nickel was sintered after 120 h on stream in the CO<sub>2</sub> reforming. The results from TG/DTA and XRD support the same conclusion that the Ni/TiO<sub>2</sub>-Al<sub>2</sub>O<sub>3</sub> catalyst deactivation is mainly due to the Ni sintering rather than to carbon deposition in the CO<sub>2</sub> reforming.

### Conclusion

The Ni-based catalysts modified by Al<sub>2</sub>O<sub>3</sub> are efficient for the CO<sub>2</sub> reforming, despite the fact that a significant amount of carbon is formed during the reaction over Ni/TiO<sub>2</sub>-Al<sub>2</sub>O<sub>3</sub>. This catalyst exhibited high activity and stability as compared with Ni/TiO<sub>2</sub>. When Al<sub>2</sub>O<sub>3</sub> is added to the support, the formation of NiAl<sub>2</sub>O<sub>4</sub> depressed the carbon deposition over Ni/TiO<sub>2</sub>-Al<sub>2</sub>O<sub>3</sub>. It resulted in the catalyst exhibiting stable activity during

the CO<sub>2</sub> reforming. On the other hand, the presence of Ni aluminate spine decreases the carbon deposition in the Ni/TiO<sub>2</sub>-Al<sub>2</sub>O<sub>3</sub> catalysts. The results suggest that the deactivation of Ni/TiO<sub>2</sub>-Al<sub>2</sub>O<sub>3</sub> catalyst have been ascribed to Ni sintering in the catalysts will be investigated in future.

### ACKNOWLEDGEMENTS

The authors gratefully acknowledged the Fundamental Project of Shanxi Province for Study Abroad (2013-105) and the Natural Science Fund of Shanxi Province (2013011009-3) as well as Fund of Yuncheng University (CY-2012017, YQ-2013010).

### REFERENCES

1. Y. Zhang and A. Reller, *Chem. Commun.*, **6**, 606 (2002).
2. A.M. Gadalla and B. Bower, *Chem. Eng. Sci.*, **43**, 3049 (1988).
3. Y.G. Chen and J. Ren, *Catal. Lett.*, **29**, 39 (1994).
4. T. Hayakawa, S. Suzuki, J. Nakamura, T. Uchijima, S. Hamakawa, K. Suzuki, T. Shishido and K. Takehira, *Appl. Catal. A*, **183**, 273 (1999).
5. Z.L. Zhang and X.E. Verykios, *Appl. Catal. A*, **138**, 109 (1996).
6. A. Vejux and P. Courtine, *J. Solid State Chem.*, **23**, 93 (1978).
7. R.D. Shannon, *J. Appl. Phys.*, **35**, 3414 (1964).
8. T. Hayakawa, S. Suzuki, J. Nakamura, T. Uchijima, S. Hamakawa, K. Suzuki, T. Shishido and K. Takehira, *Appl. Catal. A*, **183**, 273 (1999).
9. S. Tang, L. Ji, J. Lin, H.C. Zeng, K.L. Tan and K. Li, *J. Catal.*, **194**, 424 (2000).
10. S. Wang and G.Q. Lu, *Ind. Eng. Chem. Res.*, **36**, 5103 (1997).
11. M.C.J. Bradford and M. Albert Vannice, *Catal. Today*, **50**, 87 (1999).
12. S.-C. Ho and T.-C. Chou, *Ind. Eng. Chem. Res.*, **34**, 2279 (1995).